Preparation, crystal structure and chemical bonding analysis of the new binary compounds Rh_4Ga_{21} and Rh_3Ga_{16}

Magnus Boström*, Yurii Prots, Yuri Grin

Max-Planck-Institut für Chemische Physik fester Stoffe, Nöthnitzer Straße 40, 01187 Dresden, Germany

Abstract

The two new binary compounds Rh_4Ga_{21} (space group *Cmca* (*Cmce*), $a = 40.135(6)$ Å, $b = 6.470(2)$ Å, $c = 6.473(1)$ Å, Pearson symbol *oC*136) and Rh_3Ga_{16} (space group *Ccca* (*Ccce*), $a = 30.424(7)$ Å, $b = 6.476(2)$ Å, $c = 6.468(2)$ Å, Pearson symbol *oC*76) were synthesised and their crystal structures were solved from single-crystal X-ray diffraction data. From a topological point of view, both these two crystal structures and the crystal structure of $PdGa_5$ can be described either as inhomogeneous intergrowth structures containing three different kinds of segments, or as built up by layers of capped square antiprisms condensed via their capping atoms. Bonding analysis with bonding indicators revealed that the crystal structures of Rh_4Ga_{21} and Rh_3Ga_{16} have to be considered as framework polyanions formed by covalently bonded gallium atoms with embedded rhodium cations.
© 2006 Elsevier Inc. All rights reserved.

Keywords: Binary compound; Rhodium; Gallium; Crystal structure; Electron localization function; Electron localizability indicator

1. Introduction

Four binary phases are known in the Rh–Ga system; RhGa (CsCl type, Pearson symbol *cP*2) [1], $Rh_{10}Ga_{17}$ (prototype, *tP*108) [2], $RhGa_3$ (IrIn$_3$ type [3], *tP*16) [4] and Rh_2Ga_9 (prototype, *mP*22) [5,6]. No phase diagram has hitherto been published. In course of a systematic investigation of Ga- and Al-rich compounds of Ir, several new phases were found [6,7]. This encouraged an investigation of the chemically related Rh–Ga system, of which the first results are the subject of the present work.

2. Experimental

Single crystals of Rh_4Ga_{21} were prepared in a Ga-rich self-flux containing 0.0538 g Rh (99.9%, Chempur) and 0.952 g Ga (99.999%, Chempur), hence having the nominal composition $Rh_{3.7}Ga_{96.3}$. The elements were sealed inside an evacuated quartz tube already prepared with a quartz wool filter on a support of small pieces of crushed quartz

glass according to the high-temperature centrifugation aided filtration technique (HTCAF) [8,9]. The sample was heat treated at 300 °C for 18 days before the melt was removed from the solid using a centrifuge operating at 2000*g*, without significantly decreasing the temperature of the sample.

Single crystals of Rh_3Ga_{16} were prepared analogously from 0.0239 g Rh and 1.003 g Ga (nominal composition $Rh_{1.6}Ga_{98.4}$), but cooled down from 900 °C at the rate of 5 °C/h down to 150 °C, where the sample was kept for 18 days before the melt was removed.

X-ray powder diffraction patterns of the powdered single crystals were collected with a Huber Imaging Plate Guinier Camera 670 using CuKα_1 radiation ($\lambda = 1.54059$ Å) for Rh_3Ga_{16} and CoKα_1 radiation ($\lambda = 1.78897$ Å) for Rh_4Ga_{21}. Silicon ($a = 5.43119(1)$ Å) and LaB$_6$ powder ($a = 4.15692(1)$ Å), respectively, were added as internal standard to the samples. The lattice parameters were refined from the powder data with the program CELLREF [10].

Single crystals with well-exhibited faces were isolated and parts of them were used for the X-ray diffraction experiment. Single-crystal X-ray diffraction data were

*Corresponding author. Fax: +49 351 4646 4002.
E-mail address: bostroem@cpfs.mpg.de (M. Boström).

collected on a Rigaku Mercury CCD diffraction system employing Mo$K\alpha$ radiation ($\lambda = 0.71069$ Å). The measured data sets were corrected for absorption using multi-scans in the Laue-class *mmm*. Relevant details for the data collection and handling are summarized in Table 1.

The crystal structures of Rh_4Ga_{21} and Rh_3Ga_{16} were solved by direct methods with the Shelxs97 program [11]. The refinement was performed using the program Jana2000 [12]. The refined parameters were scale factor, atomic coordinates, anisotropic displacement parameters, extinction coefficient and a twinning factor for Rh_3Ga_{16}.

The TB–LMTO–ASA program package [13] with exchange correlation potential (LDA) according to Barth and Hedin [14] was used for quantum chemical calculations. Because of the clear similarity between the crystal structures of Rh_3Ga_{16} and Rh_4Ga_{21}, the calculations were made only for the latter. The radial scalar-relativistic Dirac equation was solved to obtain the partial waves. A calculation within the atomic sphere approximation (ASA) includes corrections for the neglect of partial waves

of higher order and interstitial regions [15], hence no addition of empty spheres was found to be necessary. The radii of the atomic spheres used in the calculations were: $r(Rh1) = 1.609$ Å, $r(Rh2) = 1.630$ Å, $r(Ga1) = 1.543$ Å, $r(Ga2) = 1.537$ Å, $r(Ga3) = 1.579$ Å, $r(Ga4) = 1.581$ Å, $r(Ga5) = 1.605$ Å, $r(Ga6) = 1.597$ Å, $r(Ga7) = 1.571$ Å. A basis set containing the Rh(5s, 5p, 4d) and Ga(4s, 4p) orbitals was employed for the self-consistent calculations with the Rh(4f) and Ga(4d) functions being downfolded. The electron localization function (ELF, η) was evaluated according to [16] within the TB–LMTO–ASA program package with an ELF module already implemented. To gain a deeper insight in the chemical bonding, the topology of ELF was analysed with the program Basin [17]. The electron density was integrated in basins which were bound by zero flux surfaces in the ELF gradient. This method, analogous to the procedure proposed by Bader [18] for charge calculations from electron densities resulted in electron counts for each basin, which revealed basic information for the description of the bonding situation.

Table 1
Crystallographic information and data handling for Rh_4Ga_{21} and Rh_3Ga_{16}

	Rh_4Ga_{21}		Rh_3Ga_{16}
Crystal data			
Chemical formula	Rh_4Ga_{21}		Rh_3Ga_{16}
Crystal system		Orthorhombic	
Space group	*Cmca* (*Cmce*)		Ccca (*Ccce*)
Z	4		4
a (Å)[a]	40.135(6)		30.424(7)
b (Å)[a]	6.470(2)		6.476(2)
c (Å)[a]	6.473(1)		6.468(2)
V (Å^3)[a]	1681		1274
Density calc. (g cm^{-3})	7.41		7.42
Crystal form		Irregular	
Crystal size (mm^3)	$0.050 \times 0.040 \times 0.020$		$0.040 \times 0.030 \times 0.015$
Colour		Grey metallic	
Absorption coefficient (mm^{-1})	36.8		37.0
Data collection			
Diffraction system		Rigaku AFC7 Mercury CCD	
Radiation, λ (Å)		Mo$K\alpha$, 0.71069	
No. of measured reflections	6820		2858
Range of $h\,k\,l$	$-43 \leqslant h \leqslant 57$		$-41 \leqslant h \leqslant 41$
	$-9 \leqslant k \leqslant 9$		$-8 \leqslant k \leqslant 7$
	$-8 \leqslant l \leqslant 8$		$-6 \leqslant l \leqslant 8$
Absorption correction		Multi-scan	
T_{min}/T_{max}	0.523		0.541
R_{int}	0.055		0.045
Refinement			
Refinement on		F	
No. of independent reflections	1286		759
No. of independent observed reflections	967		565
Observation criterion		$I > 3\sigma(I)$	
No. of reflections used in refinement	1286		759
No. of parameters refined	62		47
Weighting scheme		Unit	
$R(F)_{all}$, w$R(F)_{all}$, $R(F)_{obs}$	0.053, 0.046, 0.036		0.076, 0.061, 0.060
GOF_{all}	1.0		5.0
$\Delta\rho_{max}$, $\Delta\rho_{min}$, (e Å^{-3})	2.0, -1.8		6.2, -1.9
Extinction model	Gaussian isotropic		—
Extinction coefficient	0.051(2)		—

[a]Cell parameters from powder diffraction data with internal standard.

3. Results and discussion

The crystal structure of Rh_4Ga_{21} was successfully solved by direct methods and refined in the space group *Cmca* (*Cmce*). Final residual values and further details on the refinement are listed in Table 1. Final coordinates and atomic displacement parameters are summarized in Tables 2 and 3. The interatomic distances are listed in Table 4.

Direct methods failed to solve the crystal structure of Rh_3Ga_{16}, apparently due to twinning. Since the two shorter lattice parameters are practically identical for Rh_4Ga_{21} and Rh_3Ga_{16}, it was assumed that the structures ought to be closely related. The long *a*-axis of Rh_3Ga_{16} is very close to 3/4 of the corresponding axis in Rh_4Ga_{21}. A hypothetical structure model was constructed with slabs containing three layers of condensed capped square antiprisms (instead of four as in the structure of Rh_4Ga_{21}) but otherwise completely analogous to the structure of Rh_4Ga_{21} (Fig. 1). The hypothetical structure was constructed in the space group *P*1, whereafter the highest reasonable space group *Cmca* (*Ccce*) was established using symmetry analysis using the program Platon [19] in several steps together with refinement. The twinning relation is described by a diagonal mirror plane represented by the matrix

$$\begin{bmatrix} 1 & 0 & 0 \\ 0 & 0 & 1 \\ 0 & 1 & 0 \end{bmatrix}.$$

The subsequent successful refinement verified the correctness of the model. For Rh_3Ga_{16}, the same parameters were refined as for the Rh_4Ga_{21} structure, except for that no extinction was refined. An additional parameter for twinning was refined to be 0.353(9). Further details of the

Table 4
Interatomic distances in Rh_4Ga_{21}

Atoms	Distance (Å)
Rh1–Ga1	2.4251(9)
Rh1–Ga2	2.421(2)
Rh1–Ga4	2.678(1)
Rh1–Ga4	2.679(1)
Rh1–Ga5	2.658(1)
Rh2–Ga2	2.446(2)
Rh2–Ga3	2.463(2)
Rh2–Ga6	2.730(1)
Rh2–Ga6	2.736(1)
Rh2–Ga7	2.587(1)
Rh2–Ga7	2.583(1)
Ga1–Ga4	2.824(1)
Ga1–Ga4	2.825(1)
Ga2–Ga5	2.835(1)
Ga2–Ga5	2.836(1)
Ga2–Ga6	2.792(1)
Ga2–Ga6	2.798(1)
Ga3–Ga7	2.896(1)
Ga3–Ga7	2.593(2)
Ga3–Ga7	2.893(1)
Ga4–Ga4	2.757(2)
Ga4–Ga4	2.738(2)
Ga4–Ga5	2.833(2)
Ga4–Ga5	2.745(2)
Ga5–Ga5	2.775(2)
Ga5–Ga6	2.706(2)
Ga6–Ga6	2.672(2)
Ga6–Ga7	2.849(2)
Ga6–Ga7	2.850(2)
Ga6–Ga7	2.697(2)
Ga7–Ga7	2.950(2)

Table 2
Final atomic parameters for Rh_4Ga_{21}

Atom	Site	x	y	z	U_{eq} [a]
Rh1	8	0.43958(2)	0	0.5	0.0065(2)
Rh2	8	0.31831(2)	0	0.5	0.0076(2)
Ga1	4	0.5	0	0.5	0.0194(6)
Ga2	8	0.37924(4)	0	0.5	0.0196(5)
Ga3	8	0.25693(4)	0	0.5	0.0238(5)
Ga4	16	0.46565(3)	0.3504(2)	0.3505(2)	0.0125(3)
Ga5	16	0.41443(3)	0.3484(2)	0.6516(2)	0.0128(3)
Ga6	16	0.34701(3)	0.3537(2)	0.6456(2)	0.0131(3)
Ga7	16	0.29621(3)	0.3391(2)	0.3386(2)	0.0159(3)

[a] $U_{eq} = 1/3\sum_i\sum_j U_{ij}a_i^*a_j^*a_ia_j$.

Table 3
Anisotropic atomic displacement parameters for Rh_4Ga_{21} [a]

Atom	U_{11}	U_{22}	U_{33}	U_{12}	U_{13}	U_{23}
Rh1	0.0052(4)	0.0069(4)	0.0076(4)	0	0	−0.0002(3)
Rh2	0.0060(4)	0.0091(4)	0.0076(4)	0	0	0.0005(3)
Ga1	0.0046(8)	0.024(2)	0.029(1)	0	0	0.001(1)
Ga2	0.0056(6)	0.0249(8)	0.0281(9)	0	0	0.0015(7)
Ga3	0.0049(7)	0.036(1)	0.0308(9)	0	0	−0.0056(8)
Ga4	0.0122(5)	0.0121(5)	0.0131(5)	−0.0002(4)	−0.0003(4)	0.0025(4)
Ga5	0.0117(5)	0.0136(5)	0.0131(5)	0.0000(4)	−0.0003(4)	−0.0022(4)
Ga6	0.0108(5)	0.0140(5)	0.0144(5)	0.0000(4)	0.0001(4)	−0.0002(4)
Ga7	0.0196(6)	0.0147(5)	0.0135(5)	0.0050(4)	0.0047(4)	0.0050(4)

[a] The total displacement factor is calculated as $\exp[-2\pi^2(U_{11}h^2a^{*2} + U_{22}k^2b^{*2} + U_{33}l^2c^{*2} + U_{12}hka^*b^* + U_{13}hla^*c^* + U_{23}klb^*c^*)]$.

Table 5
Final atomic parameters for Rh_3Ga_{16}

Atom	Site	x	y	z	U_{eq}[a]
Rh1	4	0	0.5	0	0.0072(8)
Rh2	8	0.15982(4)	0.5	0	0.0102(7)
Ga1	8	0.07958(6)	0.5	0	0.020(2)
Ga2	8	0.24074(7)	0.5	0	0.028(2)
Ga3	16	0.03356(5)	0.3493(3)	0.3483(3)	0.0134(6)
Ga4	16	0.18943(6)	0.3382(3)	−0.3390(3)	0.0194(6)
Ga5	16	0.12236(5)	0.1456(3)	−0.1460(3)	0.0152(6)

[a] $U_{eq} = 1/3\sum_i\sum_j U_{ij}a_i^*a_j^*a_ia_j$.

segments are necessary for the complete description of the symmetry, unit cell parameters and composition of the possible intermediate crystal structures, hence this is an example of so-called inhomogeneous intergrowth. The first kind of segments (Fig. 1, top left) has a composition $2 \times TE_2$ (T = transition metal, E = Al or Ga) and represents half the unit cell of the prototype structure $CuAl_2$ (space group $I4/mcm$, $a = 7.067(1)$ Å, $c = 4.877(1)$ Å, Pearson symbol $tI12$) [24–26]. The second one (Fig. 1, top middle) can be understood as an emptied U_3Si_2 structure [27]: $2 \times Si_2U_3 \rightarrow 2 \times \square_2E_3$. Both mentioned fragments have tetragonal minimal symmetry complex [23], thus the structure containing only these two types of segments ($PdGa_5$) is also tetragonal. The last type of the segments (Fig. 1, top right) can also be derived from the structure of U_3Si_2 and has a composition of $2 \times E_4$. Stacking sequences of the segments in the crystal structures of $PdGa_5$, Rh_3Ga_{16} and Rh_4Ga_{21} are shown in Fig. 1, bottom. The compositions of the unit cells can be calculated as

$$4TE_2 + 4E_3 = T_4E_{20} = 4TE_5 \text{ for } PdGa_5,$$

$$16TE_2 + 12E_3 + 4E_4 = T_{16}E_{84} = 4T_4E_{21} \text{ for } Rh_4Ga_{21},$$

$$12TE_2 + 12E_3 + 4E_4 = T_{12}E_{64} = 4T_3E_{16} \text{ for } Rh_3Ga_{16}.$$

In all three crystal structures discussed above, transition metal atoms have a square antiprismatic environment formed by Ga atoms (Fig. 1). Two additional Ga atoms cap the square faces of the antiprisms, resulting in the coordination number 10 around the rhodium atoms. In the title compounds, the antiprisms are sharing the capping atoms along the stacking axis and in this way form chains. The chains are further condensed sharing a half of the side edges, in the same way as in the $PdGa_5$ structure type. In the $PdGa_5$ structure the chains are infinite. The chains in the rhodium gallides are split in three- (Rh_3Ga_{16}) or four-membered (Rh_4Ga_{21}) fragments. The neighboring fragments are shifted by $(0, \frac{1}{2}, 0)$. With this kind of description the compositions of the unit cells for $PdGa_5$, Rh_3Ga_{16} and Rh_4Ga_{21} can be obtained as

$$[TE_{8/2}^{ap}E_{2/2}^s]_4 = 4TE_5,$$

Fig. 1. Three kinds of structural segments (top) and crystal structures of $PdGa_5$, Rh_4Ga_{21} and Rh_3Ga_{16} as intergrowth derivatives (bottom) Arrangement of condensed capped antiprisms $[PdGa_{10}]$ are highlighted. The arrows indicate which atoms are considered in the segment formulas.

refinement and final atomic parameters are summarized in Tables 5 and 6. The corresponding interatomic distances are found in Table 7.

Both crystal structures, Rh_3Ga_{16} and Rh_4Ga_{21}, represent new structure types for intermetallic compounds. They can both be related to the archetype $PdGa_5$ [3,20], (space group $I4/mcm$, $a = 6.436(6)$ Å, $c = 9.990(8)$ Å, Pearson symbol $tI10$), cf. Fig. 1. This group of intermetallic compounds can be interpreted within the concept of intergrowth structures [21–23]. In this case three different

Table 6
Anisotropic atomic displacement parameters for Rh_3Ga_{16}[a]

Atom	U_{11}	U_{22}	U_{33}	U_{12}	U_{13}	U_{23}
Rh1	0.0105(7)	0.006(2)	0.005(2)	0	0	0
Rh2	0.0120(5)	0.009(2)	0.009(2)	0	0	0.0004(5)
Ga1	0.0099(8)	0.026(3)	0.024(3)	0	0	0.000(2)
Ga2	0.0109(9)	0.046(3)	0.028(2)	0	0	0.009(2)
Ga3	0.0173(7)	0.011(2)	0.012(2)	0.0009(6)	−0.0014(6)	0.0028(6)
Ga4	0.0263(8)	0.014(2)	0.017(2)	−0.0062(8)	0.0044(7)	−0.0053(6)
Ga5	0.0176(7)	0.013(2)	0.015(2)	0.0002(6)	0.0000(6)	0.0002(6)

[a]The total displacement factor is calculated as $\exp[-2\pi^2(U_{11}h^2a^{*2} + U_{22}k^2b^{*2} + U_{33}l^2c^{*2} + U_{12}hka^*b^* + U_{13}hla^*c^* + U_{23}klb^*c^*)]$.

Table 7
Interatomic distances in Rh_3Ga_{16}

Atoms	Distance (Å)
Rh1–Ga1	2.421(2)
Rh1–Ga3	2.659(2)
Rh1–Ga3	2.669(2)
Rh2–Ga1	2.441(2)
Rh2–Ga2	2.462(2)
Rh2–Ga4	2.591(2)
Rh2–Ga4	2.587(2)
Rh2–Ga5	2.731(2)
Rh2–Ga5	2.726(2)
Ga1–Ga3	2.826(2)
Ga1–Ga3	2.835(2)
Ga1–Ga5	2.802(2)
Ga1–Ga5	2.797(2)
Ga4–Ga4	2.955(3)
Ga4–Ga5	2.697(3)
Ga4–Ga5	2.852(3)
Ga4–Ga5	2.849(3)
Ga5–Ga5	2.669(3)

$$[TE^{ap}_{8/2}E^s_{2/2}]_4[TE^{ap}_{8/2}E^s_{1/2}E^{us}]_8 = 4T_3E_{16},$$

$$[TE^{ap}_{8/2}E^s_{2/2}]_8[TE^{ap}_{8/2}E^s_{1/2}E^{us}]_8 = 4T_4E_{21},$$

where the denominator 2 implies that the atom is shared; ap = antiprism, s = shared apex, us = unshared apex. Breaking the chains together with a shift along [010] and/or [001] (coordinate system of Rh_3Ga_{16} and Rh_4Ga_{21}) leads to a reduction of the total symmetry from tetragonal to orthorhombic and is obviously the reason for twinning of the single crystals of Rh_3Ga_{16}. Nevertheless the two shorter lattice parameters in both the rhodium gallides are equal within 2 standard deviations.

The chain arrangement of TE_{10} polyhedra results in the formation of "empty" space between the chains. In the $PdGa_5$ as well as in the $CuAl_2$ structures, a covalent interaction between the antiprisms takes place in this "empty" space [26,28]. This was taken as a starting point for the bonding analysis of the compounds Rh_4Ga_{21} and Rh_3Ga_{16}.

The electron localization function (ELF) was chosen as a suitable tool for this investigation. Originally introduced by Becke and Edgcombe within the Hartree–Fock theory [29] and redefined later by Savin et al. [16] for the density functional theory, the electron localization function belongs to the so-called bonding indicators in real space. Functions of this group trace the correlation of electronic motion of same-spin electrons. A more general functional of this kind is called electron localization indicator (ELI) [30]. ELF (as an approximation of ELI) represents a charge distribution of electron pairs and is thus a suitable tool for analysis of chemical bonding in the sense of Lewis theory, where pair formation plays the central role. Maxima of ELF (and ELI) in the valence region provide signatures for directed (covalent) bonding in real space.

Some of the interatomic Rh–Ga distances (2.41–2.47 Å, Tables 4 and 7) are very short in comparison with the sum of radii ($r_{met}(Rh) = 1.34$ Å, $r_{met}(Ga) = 1.22$ Å, $r_{cov}(Rh) = 1.25$, $r_{cov}(Ga) = 1.25$ Å [31]). Despite this fact, no unique ELF attractors were found on the Rh–Ga contacts inside the polyhedra in the crystal structure of Rh_4Ga_{21}.

Topological analysis of the electron localization function revealed attractors (function maxima) which were located mostly on the Ga–Ga contacts (two-centre bonds) and can be classified in five different groups (Fig. 2, left). The attractors of the first kind are located in the "empty" space between the gallium atoms of neighboring chains (Ga3–Ga3, Ga4–Ga4 and Ga6–Ga6 bonds), similar to the bonding picture in $PdGa_5$ and $CuAl_2$. Also the second group of attractors was found outside the antiprisms, namely between the unshared Ga atoms capping the antiprisms of neighboring chain fragments (three-centre bonds Ga6–Ga7–Ga6). Attractors of a third kind were observed on the Ga–Ga contacts constituting the side edges between adjacent triangular faces of the antiprisms (two-center bonds Ga3–Ga4, Ga5–Ga6). The next group of attractors is located between capping Ga atoms and
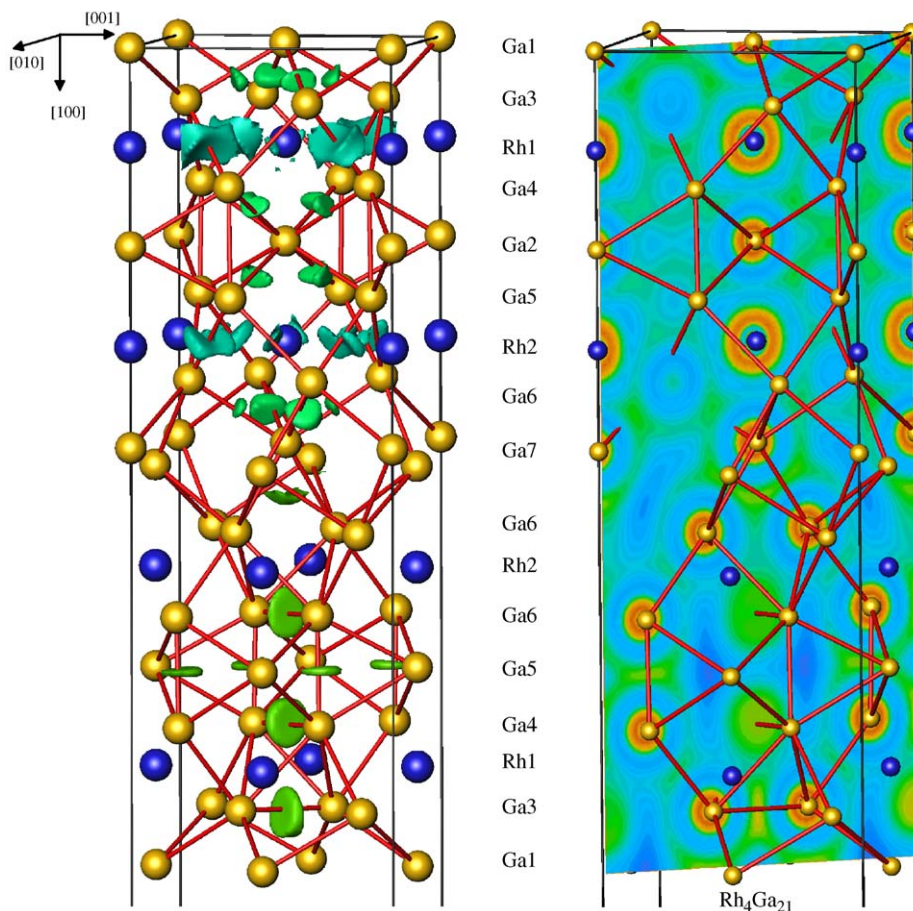
Fig. 2. Electron localization function of the crystal structure of Rh_4Ga_{21}: (left) isosurfaces of ELF showing the positions of the attractors of the Ga–Ga contacts. (right) ELF distribution on the (011) plane revealing the non-structurized spherical topology of ELF in the penultimate shell of rhodium and gallium atoms and the absence of attractors on the Rh–Ga contacts.

Ga atoms on the side edges of the $[TE_{10}]$ polyhedron (two-center bonds Ga1–Ga3, Ga4–Ga2, Ga2–Ga5, Ga6–Ga7). Attractors of the last group are situated on the bonds between antiprisms belonging to the same chain (Ga4–Ga6 bonds).

Integration of the electron density within the basins of ELF attractors gave counts of $43.8 \approx 44$ electrons for the inner shells of the crystallographically independent rhodium atoms, indicating the configuration Rh^{1+}. Based on the ELF/electron density approach, the crystal structures of Rh_4Ga_{21} and Rh_3Ga_{16} should be described as a covalently bonded network of Ga atoms forming capped square-antiprismatic cages, each containing a Rh atom (Fig. 3). The interaction between the Rh atoms and the Ga network is rather a Coulomb one, with the valence electrons of Rh transferred to the network according to the balances $(Rh^{1+})_4(Ga_{21})^{4-}$ or $(Rh^{1+})_3(Ga_{15})^{3-}$.

The formation of covalent bonds in the "empty" part of the structure between Ga (Al) atoms (i) belonging to the neighboring antiprisms and (ii) forming the side edges of the antiprisms were also observed in the two archetype structures $PdGa_5$ and $CuAl_2$. However, in contrary to the case of Rh_4Ga_{21}, a directed (covalent) interaction between the transition metal (Pd, Ga) and the Ga (Al) atoms was found in the ELF of both $PdGa_5$ and $CuAl_2$.

4. Conclusions

The two new binary compounds Rh_4Ga_{21} and Rh_3Ga_{16} were prepared in single-crystalline form and structurally characterized. In both crystal structures, as well as in $PdGa_5$, the transition metal atoms are 10-coordinated by gallium. From the bonding analysis, the new compounds are described as framework gallium polyanions with rhodium cations embedded in the tetragonal antiprismatic cavities, according to the electronic balances $(Rh^{1+})_4(Ga_{21})^{4-}$ or $(Rh^{1+})_3(Ga_{15})^{3-}$.

Further details of the crystal structure investigation can be obtained from Fachinformationszentrum Karlsruhe, 76344 Eggenstein-Leopoldshafen, Germany, (fax: +49 7247 808 666; e-mail: crysdata@fiz.karlsruhe.de) on quoting the depository number CSD 415870 for Rh_4Ga_{21} and CSD 415871 for Rh_3Ga_{16}.
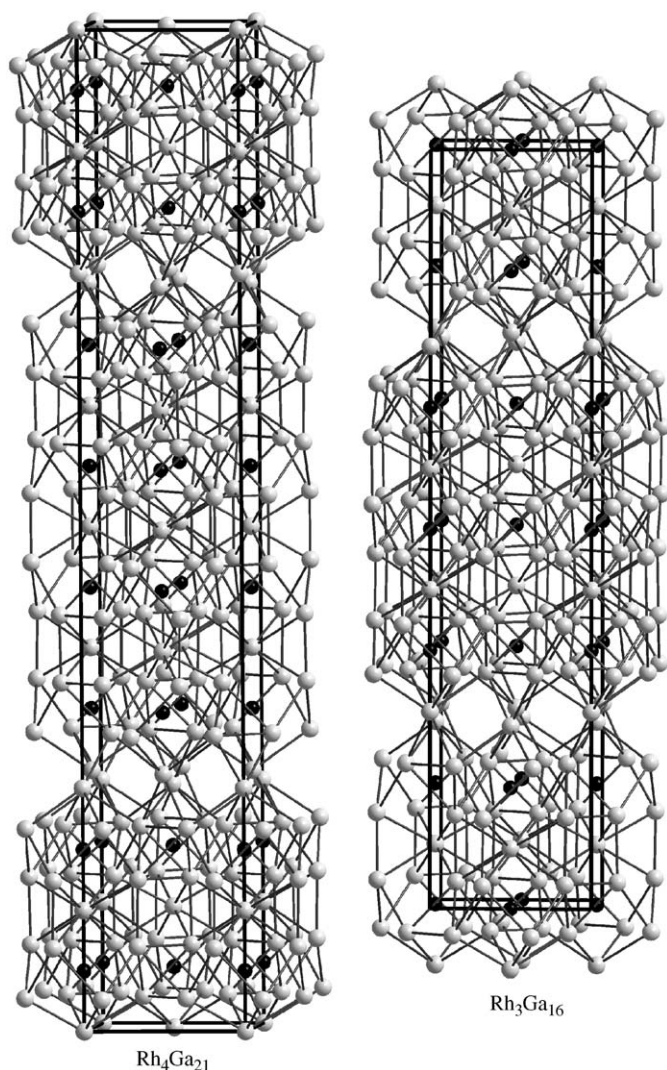
Fig. 3. Anionic gallium frameworks with embedded rhodium cations in the crystal structure of Rh_4Ga_{21} and Rh_3Ga_{16} as revealed by the analysis of the chemical bonding.

References

[1] B.H. Verbeek, H.W.A.M. Rompa, P.K. Larsen, M.S. Methfessel, F.M. Mueller, Phys. Rev. B 28 (1983) 6774–6779.

[2] H. Völlenkle, A. Wittmann, H. Nowotny, Monatsh. Chem. 98 (1967) 176–183.

[3] K. Schubert, H.L. Lukas, H.G. Meissner, S. Bhan, Z. Metallkd. 50 (1959) 534–540.

[4] K. Schubert, H. Breimer, R. Gohle, H.L. Lukas, H.G. Meissner, E. Stolz, Naturwissenschaften 45 (1958) 360–361.

[5] L.E. Edshammar, Acta Chem. Scand. 24 (1970) 1457–1458.

[6] M. Boström, H. Rosner, Y. Prots, U. Burkhardt, Y. Grin, Z. Allg. Anorg. Chem. 631 (2005) 534–541.

[7] M. Boström, Y. Prots, Y. Grin, Solid State Sci. 6 (2004) 499–503.

[8] Z. Fisk, J.P. Remeika, in: K.A. Gschneider, L.R. Eyring (Eds.) Handbook on the Physics and Chemistry of the Rare Earths, vol. 12, North-Holland, Amsterdam, 1989, p. 53.

[9] M. Boström, S. Hovmöller, J. Alloys Compd. 314 (2001) 154–159.

[10] J. Laugier, B. Bochu, CELLREF, Laboratoire des Materiaux et du Génie Physique de l'Ecole Supérieure de Physique de Grenoble, France, 2003.

[11] G.M. Sheldrick, SHELXS97–A Program for Automatic Solution of Crystal Structures, University of Göttingen, Germany, 1997.

[12] V. Petricek, M. Dusek, Jana2000. The Crystallographic Computing System, Institute of Physics, Praha, Czech Republic, 2000.

[13] O. Jepsen, A. Burkhardt, O.K. Andersen, The Program TB–LMTO–ASA. Version 4.7, Max-Planck-Institut für Festkörperforschung, Stuttgart, 1999.

[14] U. Barth, L. Hedin, J. Phys. C 5 (1972) 1629–1642.

[15] O.K. Andersen, Phys. Rev. B 12 (1975) 3060–3083.

[16] A. Savin, H.J. Flad, J. Flad, H. Preuss, H.G. von Schnering, Angew. Chem. 104 (1992) 185;
A. Savin, H.J. Flad, J. Flad, H. Preuss, H.G. von Schnering, Angew. Chem. Int. Ed. Engl. 31 (1992) 185–187.

[17] M. Kohout, Basin. Version 3.1, Max-Planck-Institut für Chemische Physik fester Stoffe, Dresden, Germany, 2005.

[18] R.F.W. Bader, Atoms in Molecules: A Quantum Theory, Oxford University Press, Oxford, 1999.

[19] A.L. Spek, J. Appl. Crystallogr. 36 (2003) 7–13.

[20] Yu. Grin, K. Peters, H.G. von Schnering, Z. Kristallogr. NCS. 212 (1997) 6.

[21] Yu. Grin, Ya.P. Yarmolyuk, E.I. Gladyshevski, Kristallografia 27 (1982) 686–692;
Yu. Grin, Ya.P. Yarmolyuk, E.I. Gladyshevski, Sov. Phys. Crystallogr. 27 (4) (1982) 413–418.

[22] E. Parthé, B. Chabot, K. Cenzual, Chimia 39 (1985) 164–174.

[23] Yu. Grin, in: E. Parthé (Ed.), Modern Perspectives in Inorganic Crystal Chemistry, Kluwer Academic Publishers, Dordrecht, The Netherlands, 1992, pp. 77–95.

[24] J.B. Friauf, J. Amer. Chem. Soc. 49 (1927) 3107–3114.

[25] A. Meetsma, J.L. de Boer, S. van Smaalen, J. Solid State Chem. 83 (1989) 370–372.

[26] Yu. Grin, F.R. Wagner, M. Kohout, M. Armbrüster, A. Leithe-Jasper, U. Wedig, H.G. von Schnering, J. Solid State Chem. (2005) accepted for publication.

[27] W.H. Zachariasen, Acta Crystallogr. 1 (1948) 265–268.

[28] Yu. Grin, U. Wedig, F. Wagner, H.G. von Schnering, A. Savin, J. Alloys Compd. 255 (1997) 203–208.

[29] A.D. Becke, K.E. Edgecombe, J. Chem. Phys. 92 (1990) 5397–5403.

[30] M. Kohout, Int. J. Quantum Chem. 97 (2004) 651–658.

[31] J. Emsley, The Elements, Oxford University Press, Oxford, 2000.